

LOW PERMEABILITY MEASUREMENTS: INSIGHTS

Sandra Profice, Gérald Hamon and Benjamin Nicot
TOTAL CSTJF – Avenue Larribau – 64018 Pau Cedex – France

This paper was prepared for presentation at the International Symposium of the Society of Core Analysts held in St. John's Newfoundland and Labrador, Canada, 16-21 August, 2015

ABSTRACT

An accurate determination of the intrinsic permeability k_l is essential for characterizing hydrocarbon production from shale. However, recent studies have reported unacceptable discrepancies (up to several decades) between k_l measurements obtained by different laboratories. These discrepancies could be explained by:

- i. The diversity of experimental protocols, since no standards of measurement have been clearly defined for poorly permeable samples.
- ii. The validity of interpretative models, which are rarely published.

Firstly, this paper presents the results of an experimental study comparing:

- i. Values of the intrinsic permeability k_l from Step Decay (gas), Pulse Decay (gas) and steady-state (both gas and liquid) tests
- ii. Values of the Klinkenberg coefficient b from Step Decay and steady-state tests
- iii. Values of the porosity ϕ from Step Decay and pycnometry tests.

On a homogeneous material principally composed of clay (pyrophyllite, $10 \text{ nD} < k_l < 60 \text{ nD}$), no matter which property is being measured (k_l , b or ϕ), different testing techniques achieve similar results. Thus, our Step Decay method provides simultaneous and accurate estimations of low porosities (ϕ down to 2 %) and permeabilities (k_l down to 10 nD). Besides, the accurate prediction of gas flow behavior by the Step Decay and steady-state interpretative models proves the relevance of the Darcy-Klinkenberg equation. In other words, gas flows in tight rock can be described as viscous flows with slippage at pore walls. To check these conclusions for reservoir rocks, the study was repeated on shale.

Secondly, we provide the results of a Round-robin test where Total and three commercial laboratories performed unsteady-state and, when possible, steady-state measurements on identical plugs of pyrophyllite. All laboratories chose their techniques and experimental conditions but had to work on the whole plugs at a given effective pressure, to provide estimations of k_l . Furthermore, no prior treatment was carried out on the plugs in order to prevent any bias in the results due to preparation. The comparison of the collected series of k_l values reveals that the results agree in a satisfactory manner.

Thus, after showing the validity of the classical interpretative models through preliminary studies on pyrophyllite and shales, the results of the round robin test emphasize the need to properly define experimental procedures in order to provide a framework in which to compare low permeability results produced by different laboratories.

INTRODUCTION

Oil and gas shales have become over the past ten years a topic of real interest due to the large amounts of hydrocarbons they could potentially produce. Their characterization is a challenging task since these unconventional reservoirs have tight pore throats (a few tens of nanometers) and low permeabilities (from microdarcies to nanodarcies). Consequently, shales require careful identification of tractable and reliable methods to identify their one-phase flow properties.

Steady-state techniques are the oldest and simplest ones. They allow the determination of the intrinsic permeability k_i and, when applied with gas at different mean pore pressures, provide the Klinkenberg coefficient b in addition [1, 2]. Until recently, the principal drawback of such methods lay in the time needed to achieve steady-state at each new measuring point. The sample characterization used to be a long process, requiring several hours or even days when the material was extremely tight. Alternative methods dedicated to a faster analysis of ultra-low permeable porous media have been developed since the early 50's. Bruce *et al.* [3] were the first authors to propose in 1953 an unsteady-state technique commonly referred to as "Pulse Decay". This pioneering work gave birth to numerous other studies on the technique, mainly aiming at deriving interpretative models [4, 5, 6]. To summarize, in most of the studies, k , apparent permeability, or k_l is estimated separately from the porosity ϕ and, in rare cases, simultaneously with b . The Pulse Decay technique is still widely used in the petroleum industry, either on core plugs or on drill cuttings. This cheaper and faster option consisting in working on cuttings, known as "Gas Research Institute (GRI) technique", was first described by Luffel and Guidry in 1992 [7]. Even if unsteady-state methods relying on the application of a pulse of pressure are popular, they are not the only methods enabling a rapid and accurate characterization of low permeable rocks. Indeed, some oil and gas companies have made the choice to be equipped with different in-house techniques such as the improved steady-state technique proposed by IFPEN [2], the "Step Decay technique" [8] developed by Total or the "Pore Pressure Oscillation technique" [9] adopted by Shell. The first technique allows a fast estimation of k_l with a liquid. The second one delivers k_l , b and ϕ simultaneously using a series of pulses of pressure to excite the plug while the last one provides k and ϕ (b too if several tests are done) using a sinusoidal pressure wave.

All techniques presented in the previous paragraph involve interpretative models based on the first assumption that Darcy's law is still valid when modeling fluid flows in poorly permeable porous media. The second assumption that Klinkenberg's law [10] is valid too is made when b is determined. However, many publications question these assumptions since the Knudsen numbers typical of shales are out of the range of validity of the Darcy-Klinkenberg law. Karniadakis and Beskok [11] and also Javadpour [12], who worked on networks composed of micropores and nanopores respectively, rejected Darcy's law and suggested new formulations of the gas flow rate. Javadpour even derived an expression of k depending not only on the material specificities but also on the fluid properties at given values of temperature and pressure. In his approach, the notion of intrinsic permeability is completely lost. Using Karniadakis and Beskok's theory, Civan [13] found a relationship

between k and k_l applicable to the whole Knudsen number range. More recently, Fathi *et al.* [14] have determined a similar relationship by theorizing the phenomenon of double molecular slippage at the pore scale.

From these last studies, a natural question arises. Are interpretative models relying on the Darcy-Klinkenberg law well-suited for shales? This is the first question this paper will try to answer. The second question regards the great number of methods used in the industry for routine measurements. Are the discrepancies between the results found on an identical sample by different laboratories explained by the diversity of their interpretative models? Indeed, several authors [15, 16] recently mentioned discrepancies between permeability estimations up to several decades. The question remains whether this wide dispersion of results is due to interpretation or to sample preparation.

STUDY

Three experimental studies were devised to answer the questions above. Study 1 aimed at comparing the values of k_l , b and ϕ estimated for homogeneous plugs of pyrophyllite with common methods of the industry to those estimated with our Step Decay method. To be more precise, the comparison was made between:

- i. The values of k_l given by a Step Decay test, a Pulse Decay test, a steady-state test with gas and a steady-state test with oil
- ii. The values of b given by a Step Decay test and a steady-state test with gas
- iii. The values of ϕ given by a Step Decay test and a pycnometry test.

The same approach was then applied in Study 2 to two shale plugs sourced from an actual development target area, in order to check whether the results from the pyrophyllite study could be corroborated by a similar study with reservoir rocks. Study 3 was a Round-robin test involving three commercial laboratories and Total. Its goal was to identify the main cause of the discrepancies often observed between the k_l estimations found by different laboratories for an identical sample.

Plugs

Study 1 was carried out on five plugs of pyrophyllite named Pyro 1, Pyro 2, Pyro 3, Pyro 4 and Pyro 5 respectively. Pyrophyllite is a homogeneous quarry rock sourced from the United States. It is mostly composed of clay and consequently has a low permeability. All plugs were successively subjected to Step Decay tests, Pulse Decay tests and steady-state tests using gas and. Pyro 5, the least permeable of the five plugs, was also analysed with a liquid at steady-state, at the end of the experiments with gas. No special treatment, such as cleaning or drying, was performed on the pyrophyllite prior to the measurements with gas, which were conducted therefore on plugs containing some water. Before starting the steady-state experiment with liquid, Pyro 5 was saturated at 400 bar during two weeks, after having created a vacuum over a period of four days. Pyro 1, Pyro 2, Pyro 3 and Pyro 4 were the four plugs sent to each of the three commercial laboratories selected for the Round-robin test of the Study 3.

The two shales involved in Study 2, Shale 1 and Shale 2 respectively, are of different origins. Shale 1 comes from a wet gas well and Shale 2 from an oil well. Both samples were subjected to all the gas tests in native state. Step Decay, Pulse Decay and steady-state. No steady-state analysis with liquid was undertaken since the oil phase existing in the plug would have probably moved with the flow. This would have led to an estimation of k_l that was not comparable with the results derived with gas.

A Mercury Injection Capillary Pressure (MICP) analysis was carried out on a fragment of rock from the same block that provided Pyro 1. Figure 1, which shows the pore throat size distribution from the MICP analysis, reveals that the most represented pore throat radius in the material is around 20 nm. This result is in line with the range of pore radius of 10 to 40 nm found by using the Density Functional Theory (DFT) method on a crushed sample taken from the Pyro 1 block. Pores in shales are likewise characterized by radii of several tens of nanometers.

Methods and Interpretative Models

The Pulse Decay technique [4] consists in applying a pulse of pressure on one face of the plug and recording the differential pressure ΔP calculated from measurements taken at both extremes of the plug. As shown on Figure 2, the plug is confined in a Hassler sleeve core holder connected to two tanks. The pulse of pressure is prepared in the upstream tank V_0 and released at the plug entrance by opening the valve v_0 . The recording of ΔP is triggered simultaneously with the pulse emission. The downstream tank V_1 collects the gas flowing out of the plug. All Pulse Decay experiments were conducted with the “Pulse Decay Permeameter 200”, an automated device manufactured by Corelab, which works with nitrogen and at high mean pore pressure P_p to eliminate the Klinkenberg effect. P_p was initially stabilized at:

- Shale 1: 31 bar (450 psi)
- Plugs of pyrophyllite and Shale 2: 69 bar (1000 psi).

The gas flow from V_0 to V_1 , which are both around 20 cm³, is started by depressurizing V_1 until ΔP reaches 3 bar (40 psi). The effective pressure P_{eff} , defined as the difference between the confining pressure P_c and P_p , was:

- Plugs of pyrophyllite: 60 bar
- Shales: 100 bar.

The temperature was fixed at 20 °C for all our tests (unsteady-state and steady-state). The interpretation of ΔP is based on Jones’ approach described in reference [5]. Jones devised a method of calculating k_l by using an approximate analytical solution of the Pulse Decay problem that combines the traditional equations of fluid mechanics in porous materials (including Darcy’s law) and excludes the Klinkenberg effect. The solution is an infinite sum of exponentials decreasing over time. At long times, the first term predominates over the other terms. As a consequence, the curve of the logarithm of ΔP evolves linearly over time, allowing the derivation of k_l from the slope.

In the Step Decay technique [8], the plug is subjected to a series of pulses of pressure. In terms of the device, the Step Decay differs from the Pulse Decay only by the existence of an additional buffer tank V_b located at the plug entrance, as represented in Figure 3. The first pulse of pressure is prepared by filling V_0 and V_b with nitrogen. Once the selected pressure setpoint is reached, valve v_b is closed to isolate V_b from V_0 . The pulse is then emitted by opening v_0 . This operation triggers the simultaneous recording of upstream and downstream pressures, P_0 and P_1 respectively. All pulses of pressure from the second pulse are produced by pressurizing V_b and are liberated by briefly opening v_b . The pulse pressures and waiting time intervals used for the Step Decay tests were the following:

- Plugs of pyrophyllite: 6 bar – 16 min / 10 bar – 30 min / 31 bar – 5 to 15 hours
- Shale 1: 3 bar – 1 hour / 5 bar – 1.5 hours / 9 bar – 2 hours
- Shale 2: 6 bar – 15 min / 13 bar – 2 hours / 22 bar – 20 hours

For each plug, the same P_{eff} was applied for both Pulse Decay and Step Decay tests. The values of V_1 were of:

- Pyro 1, Pyro 2, Pyro 3 and Pyro 4: 8.43 cm^3
- Pyro 5, Shale 1 and Shale 2: 12.46 cm^3 .

In terms of the interpretation of the raw data, the Step Decay model assumes the validity of the Darcy-Klinkenberg law, as do most Pulse Decay models found in existing studies of experiments at low pore pressure. The Step Decay provides k_l , b and ϕ by matching a numerically simulated P_1 profile with the recorded P_1 data. Note that a particular strength of the method resides in the fact that the P_0 profile acts as an input for the interpretation. One consequence of that is the removal of V_0 from the series of parameters required for the inversion. As a result, the interpretation is only concerned with the measurement of V_1 . Regarding ϕ , as evoked in reference [8], an increase in the sensitivity of P_1 to ϕ was necessary to ensure its accurate estimation by history matching. This was achieved thanks to the technique's major strength resulting from the fact that P_0 is an input of the history matching: the modulation of the excitation. By emitting successive pulses of pressure, the phenomenon of gas accumulation occurring right after the pulse emission and creating sensitivity to ϕ is generated several times, compared to only once in a Pulse Decay test.

The results from unsteady-state experiments were compared to the results from a steady-state analysis carried out with nitrogen. In the case of Pyro 5, characterization at steady-state was also repeated with Isopar L. Figure 4 shows a diagram of a typical steady-state device. Regardless of the fluid used, one point of measurement was made by regulating P_0 and recording at steady-state P_0 , P_1 and the volume flow rate Q_v . For all tests involving nitrogen, several points were taken at increasing mean pore pressures to derive k_l and b independently. For the test with Isopar L, only one point was needed to determine k_l . The parameters chosen for the characterization with nitrogen were:

- Plugs of pyrophyllite: $40 \text{ bar} \leq P_0 \leq 70 \text{ bar}$, $P_1 = P_{\text{atm}}$ (atmospheric pressure), $P_{\text{eff}} = 60 \text{ bar}$
- Shale 1: $40 \text{ bar} \leq P_0 \leq 70 \text{ bar}$, $P_1 = P_{\text{atm}}$, $P_{\text{eff}} = 100 \text{ bar}$
- Shale 2: $6 \text{ bar} \leq P_0 \leq 11 \text{ bar}$, $P_1 = P_{\text{atm}}$, $P_{\text{eff}} = 100 \text{ bar}$.

In the steady-state test with Isopar L on Pyro 5, P_0 was set at 80 bar, P_1 at 2 bar and P_{eff} at 60 bar. The interpretation of the steady-state raw data recorded with nitrogen relies on:

$$k = k_l \left(1 + \frac{b}{P_m} \right) \quad (1)$$

In this relationship presented first by Klinkenberg [10], k is calculated from Equation 2, which was derived for an isothermal steady-state gas flow by integrating the differential form of Darcy's law including the Klinkenberg effect.

$$k = \frac{\mu L P_1 Q_V}{S P_m \Delta P} \quad (2)$$

Note that μ is the viscosity, L the length, S the cross-section area and P_m the mean pore pressure. According to Klinkenberg's law, it appears that the separate estimation of k_l and b requires the plot of k versus $1/P_m$. Indeed, this plot displays a linear behaviour with a slope equal to $k_l \cdot b$ and an intercept with the Y-axis equal to k_l . For the characterization with Isopar L, the calculation of k is immediate with Darcy's law:

$$k = \frac{\mu L Q_V}{S \Delta P} \quad (3)$$

Across all tests carried out with gas on a given plug, P_p varied approximately between 1 bar and 70 bar. For these extreme values of P_p , the mean free path λ defined by Equation 4 is in the range [1 nm - 94 nm].

$$\lambda = \frac{\mu}{P} \sqrt{\frac{\pi R T}{M}} \quad (4)$$

R is the ideal gas constant, T the absolute temperature and M the molecular mass. For such a range of λ and for pyrophyllite mean pore radius R_p of 25 nm ($10 \text{ nm} \leq R_p \leq 40 \text{ nm}$), the Knudsen number Kn derived from Equation 5 is between 0.04 and 3.8.

$$Kn = \frac{\lambda}{R_p} \quad (5)$$

Consequently, in pores having radii of a few tens of nanometers, either a slip flow regime or a transition flow regime arises, depending on the level of pressure [17]. For the latter, both Darcy's law and Klinkenberg's law are seriously put into question knowing that gas molecules collide principally with pore walls and no longer with other molecules.

Round-Robin Test

After characterization, Pyro 1, Pyro2, Pyro 3 and Pyro 4 were sent successively to three different commercial laboratories for a round Robin-test comprising unsteady-state and, when possible, steady-state experiments. The specifications emphasized conducting them with nitrogen, on the whole plugs (no crushing), by regulating P_{eff} at 60 bar and without carrying out any treatment on the plugs (cleaning or drying) in order to prevent any bias

in the results due to preparation. The laboratories were free to choose their own methods and experimental conditions (pressures, flow rates, temperature...).

Laboratory 1 performed unsteady-state tests with the Pulse Decay technique and steady-state tests following a procedure similar to ours. The interpretation of the Pulse Decay raw data relied on the methodology implemented in the Pulse Decay Permeameter 200, except that the analytical solution was not Jones' but Brace *et al.*'s [4]. The unsteady-state measurements were started by increasing P_0 by a few bars (between 2.5 and 3.5 bar), after the stabilization of P_p between 15.5 and 18 bar. V_0 and V_1 were of 58 cm^3 and 47 cm^3 respectively. Estimations of k_l were deduced from the tests. Each analysis at steady-state involved several points of measurement to enable the separate identification of k_l and b . The mean P_p chosen for a given plug varied between a few bars (from 1.5 to 4 bar) and 20 bar. Both types of test were carried out at a temperature of $24 \text{ }^\circ\text{C}$.

Laboratory 2 delivered values of k_l and b from unsteady-state experiments done with the "Automated Permeameter - 68" manufactured by Coretest Systems. P_p was initially set at 14 bar. Once equilibrium was achieved, the gas flow was started by opening v_1 . Hence, P_1 was kept at P_{atm} and P_0 , recorded in V_0 of 6 cm^3 , was the only signal introduced in the history matching procedure to obtain k_l and b . The numerical model assumed as usual the validity of Darcy's law and Klinkenberg's law. The temperature was of $20 \text{ }^\circ\text{C}$.

Laboratory 3 provided estimations of k_l from steady-state and unsteady-state analyses. Steady-state tests relied on a unique point of measurement obtained by applying a similar procedure to our own, P_1 and ΔP being of 6 bar and 5 bar respectively. The value of k was then corrected with an unknown empirical correlation to derive k_l . Unsteady-state tests used the Pulse Decay method. The plug was first pressurized at 40 bar and the pulse of pressure was then prepared by increasing P_0 to 60 bar. V_0 and V_1 were of 15 cm^3 and 13 cm^3 respectively. The model, assumptions and procedure on which the interpretation was based were not given. All tests were carried out at a temperature of $22 \text{ }^\circ\text{C}$. At the moment of writing the present paper, the results of Laboratory 3 were not available but will be presented during the conference.

RESULTS AND DISCUSSION

Results of the Comparative Studies

Table 1 lists the results of all measurements conducted on the five plugs of pyrophyllite. The estimations of ϕ given by the Step Decay method were compared to those provided by pycnometers employing helium at low pressure. The subscripts "PD", "SD", "SSG", "SSO" and "Pyc" refer to: "Pulse Decay", "Step Decay", "Steady-State Gas", "Steady-State Oil" and "Pycnometry" respectively, in Table 1 as below. Moreover, the deviation indicator $D\xi$ quantifying the discrepancy between ξ_1 and ξ_2 , both estimations of ξ ($= k_l, b$ or ϕ), and used throughout the present development has been defined as:

$$D\xi = 100 \frac{|\xi_1 - \xi_2|}{(\xi_1 + \xi_2)/2} \quad (6)$$

For Pyro 1 to Pyro 5, Dk_l derived for $k_{l,SD}$ and $k_{l,PD}$ is in the range [5 % - 17 %], against [19 % - 40 %] when calculated for $k_{l,SSG}$ and $k_{l,PD}$. Consequently, the values of k_l from experiments performed with gas, i.e. $k_{l,PD}$, $k_{l,SD}$ and $k_{l,SSG}$, agree in a satisfactory manner. As highlighted in Table 1, this agreement can be extended to estimations of k_l from tests carried out with gas and oil, at least for pyrophyllite. Indeed, in the case of Pyro 5, Dk_l determined for $k_{l,SSO}$ and $k_{l,SSG}$ is about 26 %. Regarding b and ϕ , b_{SD} compares well with b_{SSG} as well as ϕ_{SD} with ϕ_{Pyc} , Db ranging from 10 % to 43 % and $D\phi$ from 0 % to 19 %. Figure 5.a presents, for Pyro 1, the normalised difference $(P_{1,rec} - P_{1,sim}) / P_{1,rec}$ where $P_{1,rec}$ is the recorded profile P_1 and $P_{1,sim}$ the profile P_1 simulated with the Step Decay model. Similar graphs were obtained for Pyro 2 to Pyro 5. The signal is flat and centered on 0, excepted during a period of less than half an hour right after the pulse emission. Figure 6 gives an example of k plotted against $1/P_m$. This graph results from the processing of the steady-state raw data collected for Pyro 1. A similar linearity was observed for Pyro 2 to Pyro 5.

Table 2 provides the results from the experiments conducted on Shale 1 and Shale 2. As emphasized for pyrophyllite plugs, the same gas-based techniques used on shale plugs to identify a given property, k_l or b , lead to consistent estimates. Dk_l is about 9 % for Shale 1 and about 19 % for Shale 2, when comparing $k_{l,SSG}$ and the mean of $k_{l,SD}$ and $k_{l,PD}$, while Db is about 21 % for Shale 1 and about 26 % for Shale 2. The estimations of ϕ_{SD} are not available since the characterization of ϕ with the Step Decay technique is uncertain when dealing with shales. The bias in ϕ is mainly due to the fact that one major assumption of the Step Decay model, which is the homogeneity of the studied rock, is rarely respected in the presence of shales. In the case where the rock is highly heterogeneous, it has been proven with numerical simulations and practical tests that the method delivers an accurate estimation of k_l , an acceptable estimation of b and an unreliable estimation of ϕ [18].

Results of the Round Robin Test

Table 3 lists the values of k_l obtained for Pyro 1, Pyro 2, Pyro 3 and Pyro 4 by Total and by the two laboratories (Laboratory 1 and Laboratory 2) which participated in the Round-robin test and could deliver their results in time for the writing of the paper. Estimations of b were provided by some of the laboratories but are not reported here since focus was primarily on the characterization of k_l . Regarding the values of k_l measured by Laboratory 1 and by Laboratory 2 for a given plug, those obtained at unsteady-state were compared to $k_{l,SD}$ while those obtained at steady-state were compared to $k_{l,SSG}$. Dk_l ranges from 31 % to 118 % at unsteady-state and from 9 % to 27 % at steady-state, leading to a maximum discrepancy factor of 3.8. Therefore, the discrepancies noted here are much more modest than the two decades reported in the literature [15].

Discussion

As demonstrated by the first series of comparative measurements performed on the plugs of pyrophyllite, our in-house Step Decay method enables the simultaneous and accurate estimation of k_l , b and ϕ , in the case of homogeneous and low permeable media. From the tests on both pyrophyllite and shale plugs, it results that a satisfactory agreement between

the estimations of k_l found with different methods used in the industry can be achieved. This conclusion is also applicable to estimations of k_l determined by different laboratories working with their own protocols and interpretative models, as highlighted by the Round-robin test. Therefore, the discrepancies of several decades reported in references [15, 16] and noted between values of k_l derived for a same plug by different laboratories cannot be explained by the diversity of the experimental conditions selected for the design and use of the devices (pressures, flow rates, volumes...). Similarly, these discrepancies cannot be justified by the diversity of the interpretative models and of their assumptions: negligible ϕ , no Klinkenberg effect, constant gas compressibility... Consequently, the main cause of divergence of the results delivered for an identical sample by several laboratories is likely the sample preparation. This last conclusion is supported by reference [19] where Tinni *et al.* evidence the great variability of k_l according to the sample specificities when dealing with cuttings. In addition, Darcy's law and Klinkenberg's law remain usable in the case of nanoporous rocks, like pyrophyllite or shale. This is clearly proven by the linear behavior observed in Figure 6. In Figure 5.b are shown the discrepancies at short times between the recorded and simulated P_1 signals. They are due to the poor quality of the recorded response P_1 and probably to the inability of the Darcy-Klinkenberg model to predict the gas flow since the values of P_p of a few bars at short times induce Knudsen numbers higher than 0.1, i.e. out of the range of validity of the Darcy-Klinkenberg law. However, despite the fact that the model is not well-adapted to predict the flow during a short period, $k_{l,SD}$ remains reliable and accurate. Thus, the need to revise classical fluid mechanics when testing rocks of low permeability is not justified in the unsteady- and steady-state ranges of P_p considered in this paper.

CONCLUSION

Redundant estimations of k_l can be determined for an identical poorly permeable plug, by using different techniques of the industry. More precisely, steady-state and unsteady-state methods applied with gas lead to results in excellent agreement on pyrophyllite and shale. The convergence of the results from all measurements with gas and from a measurement at steady-state with a liquid is true for pyrophyllite. The verification of this last point in the case of shale is ongoing. Moreover, comparable estimations of k_l can be determined by different laboratories working with their own techniques, experimental conditions and interpretative procedures, provided that sample preparation is carefully defined. Knowing the numerous difficulties tied to the characterization of cuttings, we recommend carrying out permeability measurements on whole plugs as much as possible. Finally, Darcy's law and Klinkenberg's law remain valid when modeling gas flows in nanoporous rocks such as pyrophyllite and shale. In other words, gas flows in tight formations can be described as viscous flows with slippage at pore walls.

ACKNOWLEDGEMENTS

The financial support from Total is gratefully acknowledged. Besides, we thank Ghislain Pujol, Jean-Michel Kluska, Frédéric Plantier, Sonia Vincent-Gill and Antoine Delafargue for their contribution to the work presented in this paper.

REFERENCES

1. Rushing, J. A., Newsham, K. E., Lasswell, P. M., Cox, J. C., Blasingame, T. A., “Klinkenberg-Corrected Permeability Measurements in Tight Gas Sands: Steady-State Versus Unsteady-State Techniques”, SPE Annual Technical Conference and Exhibition, Houston, Texas, USA, 26-29 September 2004.
2. Boulin, P. F., Bretonnier, P., Gland, N., Lombard, J. M., “Contribution of the Steady-State Method to Water Permeability Measurement in Very Low Permeability Porous Media”, *Oil and Gas Science and Technology - Rev. IFP Energies nouvelles*, (2012) **67**, 3, 387-401.
3. Bruce, G. H., Peaceman, D. W., Rachford Jr., H. H., Rice, J. D., “Calculations of Unsteady-State Gas Flow Through Porous Media”, *Journal of Petroleum Technology*, (1953) **5**, 3, 79-92.
4. Brace, W. F., Walsh, J. B., Frangos, W. T., “Permeability of Granite Under High Pressure”, *Journal of Geophysical Research*, (1968) **73**, 6, 2225-2236.
5. Jones, S. C., “A Rapid Accurate Unsteady-State Klinkenberg Permeameter”, *SPE Journal*, (1972) **12**, 5, 383-397.
6. Hsieh, P. A., Tracy, J. V., Neuzil, C. E., Bredehoeft, J. D., Silliman, S. E., “A Transient Laboratory Method for Determining the Hydraulic Properties of ‘Tight’ Rocks - 1. Theory”, *International Journal of Rock Mechanics and Mining Sciences & Geomechanics Abstracts*, (1980) **18**, 3, 245-252.
7. Luffel, D. L., Guidry, F. K., “New Core Analysis Methods for Measuring Reservoir Rock Properties of Devonian Shale”, *Journal of Petroleum Technology*, (1992) **44**, 11, 1184-1190.
8. Lasseux, D., Jannot, Y., Profice, S., Mallet, M., Hamon, G., “The ‘Step Decay’: A New Transient Method for the Simultaneous Determination of Intrinsic Permeability, Klinkenberg Coefficient and Porosity on Very Tight Rocks”, International Symposium of the Society of Core Analysts, Aberdeen, Scotland, 27-30 August 2012.
9. Wang, Y., Knabe, R. J., “Permeability Characterization on Tight Gas Samples Using Pore Pressure Oscillation Method”, International Symposium of the Society of Core Analysts, Halifax, Nova Scotia, Canada, 4-7 October 2010.
10. Klinkenberg, L. J., “The Permeability of Porous Media to Liquids and Gases”, *API Drilling and Production Practice*, (1941), 200-213.
11. Karniadakis, G., Beskok, A., Aluru, N., *Microflows and Nanoflows, Fundamentals and Simulation*, Springer-Verlag, New-York, 2005, 818 p.
12. Javadpour, F., “Nanopores and Apparent Permeability of Gas Flow in Mudrocks (Shales and Siltstones)”, *Journal of Canadian Petroleum Technology Distinguished Author Series*, (2009) **48**, 8, 16-21.
13. Civan, F., “Effective Correlation of Apparent Gas Permeability in Tight Porous Media”, *Transport in Porous Media*, (2009) **82**, 2, 375-384.
14. Fathi, E., Tinni, A., Akkutlu, I. Y., “Shale Gas Correction to Klinkenberg Slip Theory”, America’s Unconventional Resources Conference, Pennsylvania, USA, 5-7 June 2012.
15. Passey, Q. R., Bohacs, K. M., Esch, W. L., Klimentidis, R., Sinah, S., “From Oil-Prone Source Rock to Gas-Producing Shale Reservoir - Geologic and Petrophysical

- Characterization of Unconventional Shale Gas-Reservoirs”, CPS/SPE International Oil & Gas Conference and Exhibition, Beijing, China, 8-10 June 2010.
16. Sondergeld, C. H., Newsham, K. E., Comisky, J. T., Rice, M. C., Rai, C. S., “Petrophysical Considerations in Evaluating and Producing Shale Gas Resources”, SPE Unconventional Gas Conference, Pittsburgh, Pennsylvania, USA, 23-25 February 2010.
 17. Ziarani, A. S., Aguilera, R., “Knudsen’s Permeability Correction for Tight Porous Media”, *Transport in Porous Media*, (2012) **91**, 1, 239-260.
 18. Profice, S., *Mesure de Propriétés Monophasiques de Milieux Poreux Peu Perméables par Voie Instationnaire*, PhD Thesis, Université de Bordeaux, France, 2014.
 19. Tinni, A. O., *Permeability Measurements of Nanoporous Rocks*, Master Thesis, University of Oklahoma, USA, 2012.

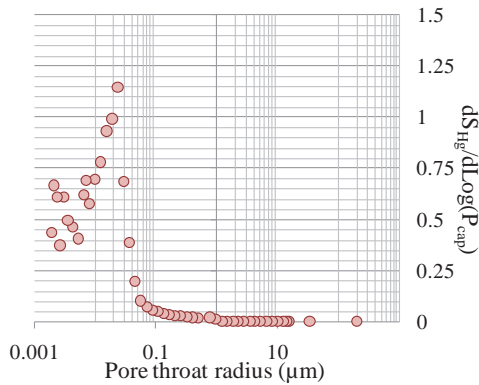


Figure 1 : Pore throat size distribution

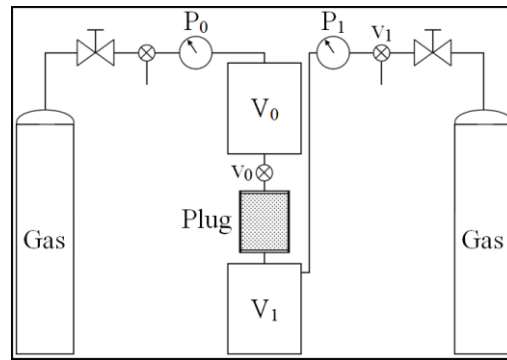


Figure 2 : Pulse Decay device

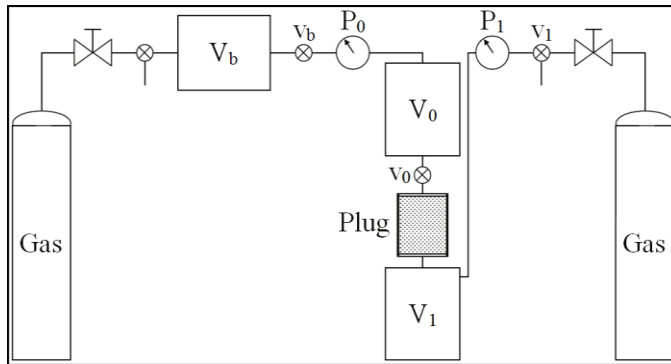


Figure 3 : Step Decay device

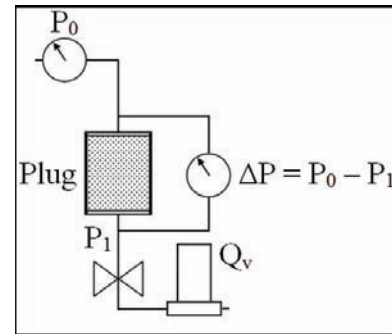


Figure 4 : Steady-state device

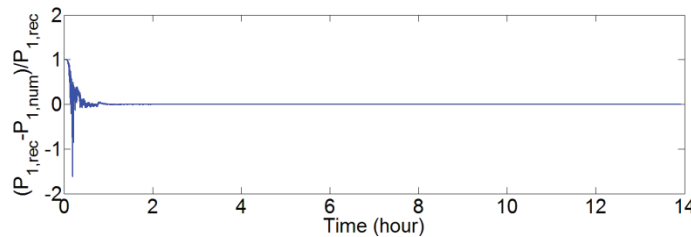


Figure 5.a : Normalised difference between $P_{1,rec}$ and $P_{1,sim}$ versus time

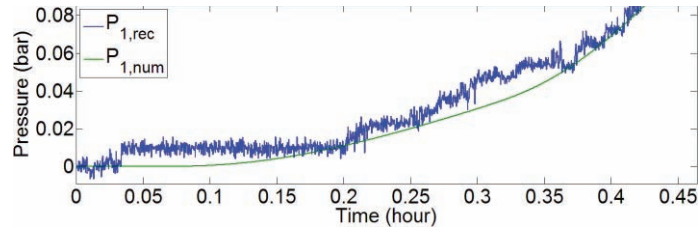


Figure 5.b : $P_{1,rec}$ and $P_{1,sim}$ signals at short times

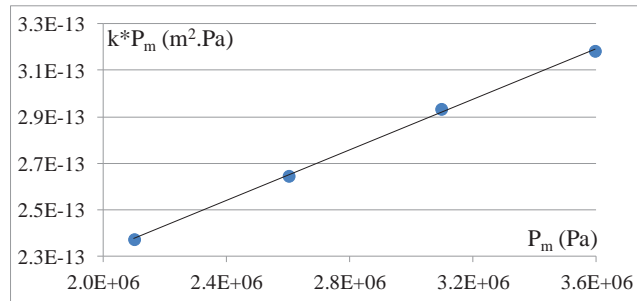


Figure 6 : $k \cdot P_m$ versus P_m

Table 1 : Results of the comparative measurements for the plugs of pyrophyllite

Plug	k_l (nD)				b (bar)		ϕ (%)	
	$k_{l,PD}$	$k_{l,SD}$	$k_{l,SSG}$	$k_{l,SSO}$	$b_{,SD}$	$b_{,SSG}$	$\phi_{,SD}$	$\phi_{,Pvc}$
Pyro 1	70	59	56	-	19.6	22.4	4.2	4.1
Pyro 2	35	33	24	-	24.0	26.6	3.8	3.5
Pyro 3	67	56	53	-	18.5	23.0	4.0	4.0
Pyro 4	51	46	42	-	20.2	24.6	3.7	3.5
Pyro 5	11	10	14	8	33.3	21.5	2.5	2.1

Table 2 : Results of the comparative measurements for the shales

Plug	k_l (nD)				b (bar)		ϕ (%)	
	$k_{l,PD}$	$k_{l,SD}$	$k_{l,SSG}$	$k_{l,SSO}$	$b_{,SD}$	$b_{,SSG}$	$\phi_{,SD}$	$\phi_{,Pvc}$
Shale 1	2031	2222	2303	-	4.3	3.5	-	10.1
Shale 2	46	58	43	-	7.4	9.6	-	0.7

Table 3 : Results of the round robin test

Plug	Total				Laboratory 1		Laboratory 2	
	k_l (nD)							
	$k_{l,PD}$	$k_{l,SD}$	$k_{l,SSG}$	$k_{l,SSO}$	$k_{l,PD}$	$k_{l,SSG}$	$k_{l,PD}$	$k_{l,SSG}$
Pyro 1	70	59	56	-	115	48	203	-
Pyro 2	35	33	24	-	45	22	127	-
Pyro 3	67	56	53	-	121	59	185	-
Pyro 4	51	46	42	-	78	55	104	-